Report

Current Biology

Conservation of the PBL-RBOH immune module in land plants

Highlights

- Chitin-induced ROS production is a conserved immune response in land plants
- MpRBOH1 and MpPBLa are required for chitin-induced ROS production in *Marchantia*
- MpRBOH1 is a *bona fide* substrate of MpPBLa

Authors

Jiashu Chu, Isabel Monte, Thomas A. DeFalco, Philipp Köster, Paul Derbyshire, Frank L.H. Menke, Cyril Zipfel

Correspondence

cyril.zipfel@botinst.uzh.ch

In brief

Rapid ROS production is a key signaling output in plant immunity. Chu et al. show that chitin-induced ROS production is conserved in the liverwort *Marchantia polymorpha* and is controlled by the MpPBLa-MpRBOH1 signaling module. MpPBLa phosphorylates MpRBOH1 at conserved residues to induce ROS production upon chitin perception.

Chu et al., 2023, Current Biology *33*, 1–8
March 27, 2023
https://doi.org/10.1016/j.cub.2023.01.050

CellPress

Please cite this article in press as: Chu et al., Conservation of the PBL-RBOH immune module in land plants, Current Biology (2023), https://doi.org/10.1016/j.cub.2023.01.050

Current Biology

CellPress
OPEN ACCESS

Report

Conservation of the PBL-RBOH immune module in land plants

Jiashu Chu,[1] Isabel Monte,[1,3] Thomas A. DeFalco,[1,4] Philipp Köster,[1] Paul Derbyshire,[2] Frank L.H. Menke,[2] and Cyril Zipfel[1,2,5,*]

[1]Institute of Plant and Microbial Biology and Zurich-Basel Plant Science Center, University of Zurich, Zurich 8008, Switzerland
[2]The Sainsbury Laboratory, University of East Anglia, Norwich Research Park, Norwich NR4 7UH, UK
[3]Present address: Center for Plant Molecular Biology (ZMBP), University of Tuebingen, Tuebingen 72076, Germany
[4]Present address: Department of Biology, Western University, London, ON N6A 5B7, Canada
[5]Lead contact
*Correspondence: cyril.zipfel@botinst.uzh.ch
https://doi.org/10.1016/j.cub.2023.01.050

SUMMARY

The rapid production of reactive oxygen species (ROS) is a key signaling output in plant immunity. In the angiosperm model species *Arabidopsis thaliana* (hereafter *Arabidopsis*), recognition of non- or altered-self elicitor patterns by cell-surface immune receptors activates the receptor-like cytoplasmic kinases (RLCKs) of the AVRPPHB SUSCEPTIBLE 1 (PBS1)-like (PBL) family, particularly BOTRYTIS-INDUCED KINASE1 (BIK1).[1–3] BIK1/PBLs in turn phosphorylate the nicotinamide adenine dinucleotide phosphate (NADPH) oxidase RESPIRATORY BURST OXIDASE HOMOLOG D (RBOHD) to induce apoplastic ROS production.[4,5] PBL and RBOH functions in plant immunity have been extensively characterized in flowering plants. Much less is known about the conservation of pattern-triggered ROS signaling pathways in non-flowering plants. In this study, we show that in the liverwort *Marchantia polymorpha* (hereafter *Marchantia*), single members of the RBOH and PBL families, namely MpRBOH1 and MpPBLa, are required for chitin-induced ROS production. MpPBLa directly interacts with and phosphorylates MpRBOH1 at specific, conserved sites within its cytosolic N terminus, and this phosphorylation is essential for chitin-induced MpRBOH1-mediated ROS production. Collectively, our work reveals the functional conservation of the PBL-RBOH module that controls pattern-triggered ROS production in land plants.

RESULTS AND DISCUSSION

To examine the conservation of reactive oxygen species (ROS) production mechanisms during land plant immune signaling, we treated the wild-type *Marchantia polymorpha* (hereafter *Marchantia*) Tak-1 with the pathogen-associated molecular patterns (PAMPs) flg22 (the 22-amino-acid peptide epitope of bacterial flagellin) or chitin (a major fungal cell wall component). It was previously shown that flg22 treatment failed to inhibit *Marchantia* gemmaling growth[6] and, similarly, *Marchantia* thalli were insensitive to flg22 treatment in terms of ROS production (Figure 1A), which is in line with the absence of an ortholog of the angiosperm flg22 receptor FLAGELLIN SENSING 2 (FLS2) in the *Marchantia* genome.[7] In contrast, chitin induced clear apoplastic ROS production in this assay (Figure 1A), consistent with the presence of lysin-motif domain-containing receptors in the *Marchantia* genome.[6,7,8] In angiosperm species, PAMP-induced ROS production depends on members of the plant nicotinamide adenine dinucleotide phosphate (NADPH) oxidase RESPIRATORY BURST OXIDASE HOMOLOG (RBOH) family.[9–14] Notably, pre-treatment with the NADPH oxidase inhibitor diphenyleneiodonium (DPI) significantly reduced chitin-induced ROS production (Figure 1A), suggesting that the RBOH-mediated ROS production machinery is conserved in *Marchantia*.

The *Marchantia* genome encodes two RBOH family members, *Mp3g20340* (Mp*RBOH1*) and *Mp7g00270* (Mp*RBOH2*). Phylogenetic analysis with RBOHs from different land plant species could not clearly establish an orthologous relationship between RBOHs from angiosperm species and those from *Marchantia* (Figure 1B). The expression of both Mp*RBOH* genes was detected in multiple tissues and development stages (Figure S1A),[15] and their mRNA levels were enhanced in response to chitin treatment, with Mp*RBOH1* displaying a stronger response—similar to that of the immune marker gene Mp*WRKY22*[6] (Figure S1B). Notably, an increase of Mp*RBOH1* transcript abundance was observed during infection with the oomycete pathogen *Phytophthora palmivora* (Figure S1A).[15] To characterize the function of MpRBOHs, we generated single knockout mutants for both family members with CRISPR-Cas9-nickase.[16,17] Two different alleles of Mp*rboh1* and two independent lines representing one allele of Mp*rboh2* were isolated, and their genotypes were confirmed by sequencing (Figures S1C and S1D). Although Mp*rboh2* plants responded normally to chitin treatment (Figure 1C), Mp*rboh1* alleles were completely incompetent of chitin-triggered ROS production (Figure 1C). ROS production in Mp*rboh1* was restored by the expression of Cas9-nickase-insensitive wild-type MpRBOH1 (Figures S1E and S1F). Among the ten-member *Arabidopsis thaliana* (hereafter *Arabidopsis*) RBOH

Please cite this article in press as: Chu et al., Conservation of the PBL-RBOH immune module in land plants, Current Biology (2023), https://doi.org/10.1016/j.cub.2023.01.050

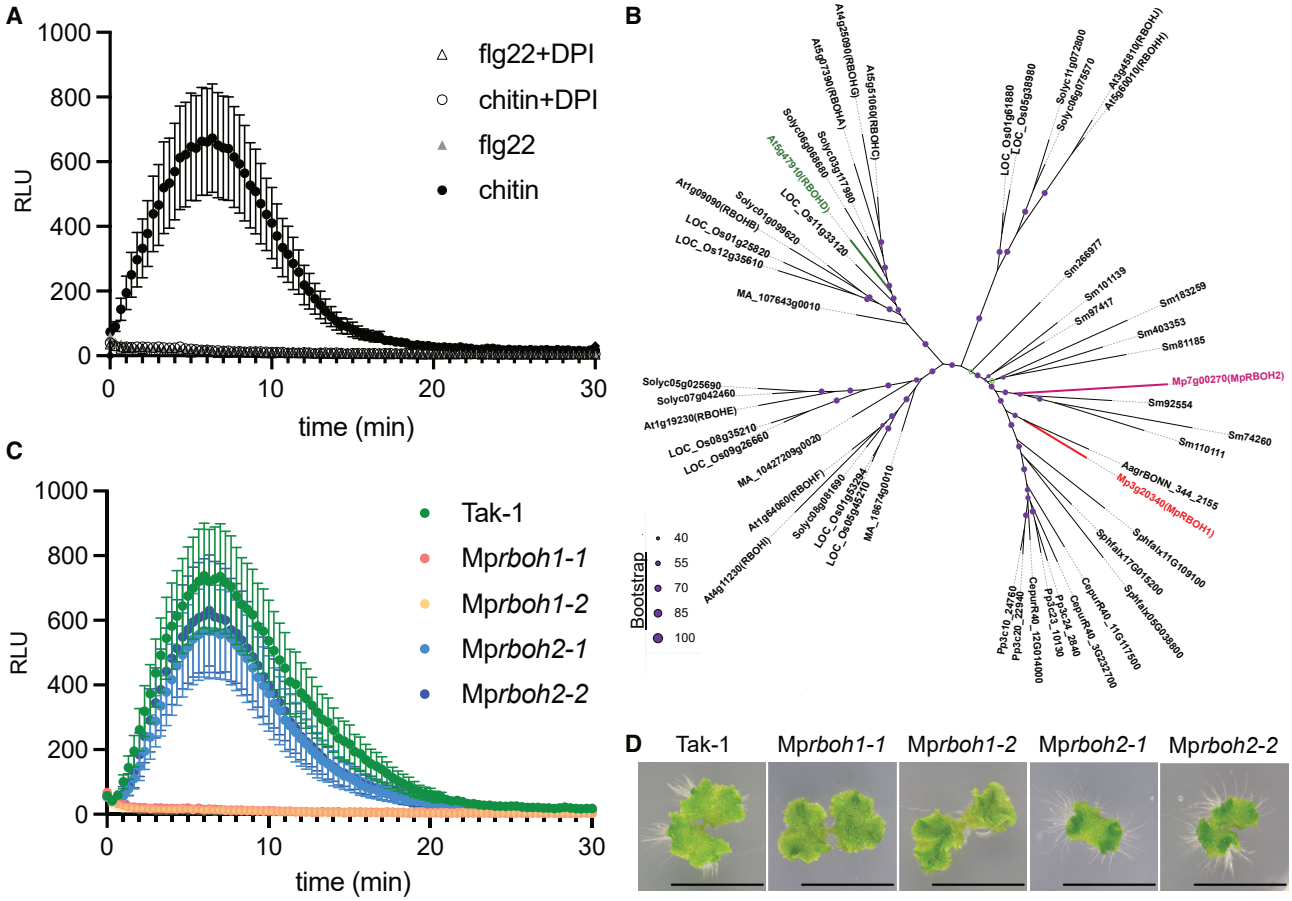

Figure 1. MpRBOH1 is required for chitin-induced ROS production in *Marchantia*

(A) Chitin (0.1 mg/mL) induces ROS production on 4-week-old *Marchantia* thallus discs in Tak-1. Discs were incubated with or without 10 μM DPI for 3 h before PAMP treatments. Values correspond to the mean of 12 samples (±SE) and are expressed in relative light units (RLUs). Experiments were performed twice with similar results.

(B) Phylogenetic analysis of RBOH family proteins from land plant species. Full-length protein sequences were aligned by MUSCLE and the unrooted phylogenetic tree were constructed using the maximum likelihood method with a 1,000 bootstrap resampling value. At, *Arabidopsis thaliana*; Solyc, *Solanum lycopersicum*; LOC_Os, *Oryza sativa*; Sm, *Selaginella moellendorffii*; MA, *Picea abies*; Sphfalx, *Sphagnum fallax*; CepurR40, *Ceratodon purpureus* R40; Pp, *Physcomitrium patens*; Mp, *Marchantia polymorpha*; AagrBONN, *Anthoceros agrestis* (Bonn). Branches that did not pass bootstrap analysis are labeled with green boxes.

(C) ROS production induction by chitin treatment (0.1 mg/mL) on 4-week-old *Marchantia* thallus discs in Tak-1 and Mp*rboh* backgrounds. Values correspond to the mean of 12 samples (±SE) and are expressed in RLU. Experiments were performed 3 times with similar results.

(D) Developmental phenotype of Mp*rboh* mutants. 12-day-old gemmalings of Tak-1, Mp*rboh1-1*, Mp*rboh2-1* grown on half-strength Gamborg's B5 1% agar medium. Scale bars, 1 cm.

See also Figure S1.

family, RBOHD is solely required for pattern-induced ROS production.[13,14] These observations suggest that in both *Marchantia* and *Arabidopsis*, a single RBOH protein is required for chitin-induced ROS production.

RBOHs are involved in multiple plant processes.[18] In addition to the chitin-induced ROS phenotype, Mp*rboh1* mutants exhibited defects in rhizoid development (Figures 1D and S1G). In contrast, Mp*rboh2* mutants exhibited strong overall defects in thallus growth, but were still able to produce rhizoids (Figures 1D, S1G, and S1H). Notably, while *Arabidopsis rbohd* mutants do not show any obvious rosette leaves or root development phenotype,[19] another *Arabidopsis* RBOH family member, RBOHC, is a positive regulator of root hair growth.[20] Rhizoids are functionally reminiscent of root hairs,[21] and both elongate by tip growth, implying that MpRBOH1 might also be involved in the regulation of tip growth in *Marchantia*.

A single PBL isoform is required for chitin-triggered ROS production in *Marchantia*

RBOH activation during immunity is controlled by several regulatory mechanisms.[22] In *Arabidopsis*, BOTRYTIS-INDUCED KINASE1 (BIK1)/PBL1-mediated phosphorylation is essential for RBOHD activation and function during pattern-triggered immunity.[4,5] We thus tested whether MpRBOH1 is similarly regulated by any of the *Marchantia* AVRPPHB SUSCEPTIBLE 1 (PBS1)-like (PBL) family proteins.

Please cite this article in press as: Chu et al., Conservation of the PBL-RBOH immune module in land plants, Current Biology (2023), https://doi.org/10.1016/j.cub.2023.01.050

CellPress
OPEN ACCESS

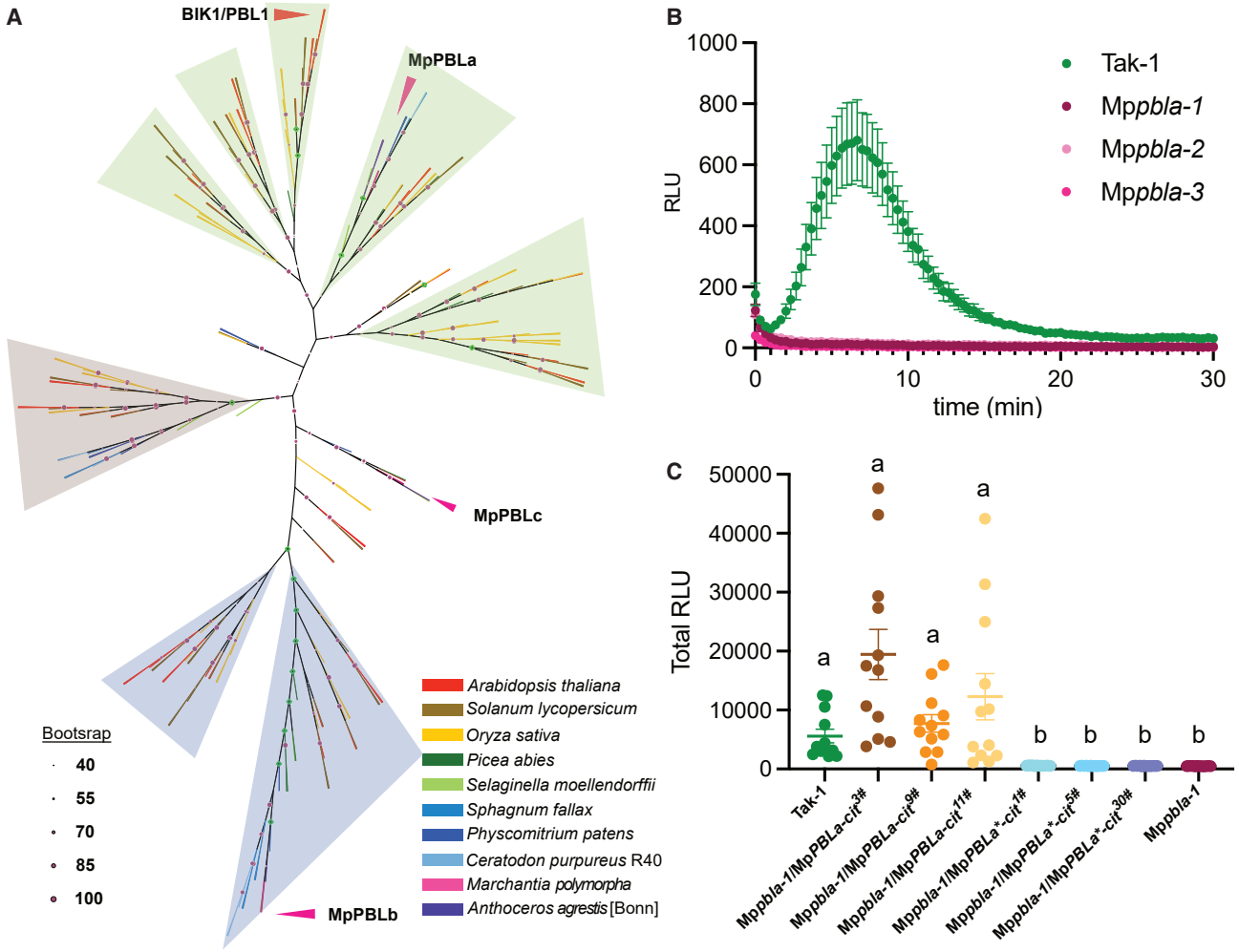

Figure 2. MpPBLa positively regulates chitin-triggered ROS production in a kinase activity-dependent manner

(A) Phylogenetic analysis of PBL family proteins from land plant species. Full-length protein sequences were aligned by MUSCLE and the unrooted phylogenetic tree was constructed using the maximum likelihood method with a 1,000 bootstrap resampling value. Branch colors represent the sequence origins. Branches that did not pass bootstrap analysis are labeled with green dots. Three major clades are highlighted with colored boxes. Phylogenetic tree with all gene identifiers is provided in Figure S4.

(B) ROS production induction by 0.1 mg/mL chitin treatment on 4-week-old *Marchantia* thallus discs in Tak-1 and Mp*ppbla* knockout mutant backgrounds. Values correspond to the mean of 12 samples (±SE) and are expressed in RLU. Experiments were performed 3 times with similar results.

(C) Chitin (0.1 mg/mL)-induced ROS production on 4-week-old *Marchantia* thallus discs in Tak-1, Mp*ppbla-1*, and Mp*ppbla-1* expressing wild-type or kinase-dead versions of MpPBLa fused with a C-terminal citrine (cit) tag under the control of the 35S promoter. Scatter plots represent the total RLU (Total RLU) over a 30-min measurement, and horizontal bars and crosses represent mean and SE, n = 12. Equal letters at the top of the panel indicate $p > 0.05$, one-way ANOVA and a Kruskal-Wallis test. Experiments were performed 3 times with similar results.

See also Figure S2.

Three PBL-encoding genes were identified in the *Marchantia* genome: *Mp3g25360* (Mp*PBLa*), *Mp3g18020* (Mp*PBLb*), and *Mp2g14830* (Mp*PBLc*).[7] Our phylogenetic analysis of PBL homologs among land plants identified three major clades dividing into eight subgroups (Figure 2A). Importantly, none of the three MpPBLs falls into the same subgroup as BIK1 or PBL1. In contrast to land plant RBOHs, MpPBLa and MpPBLb are part of clades that are present in all tested land plant species, wherein a single Mp*PBL* gene is orthologous to its bryophyte and tracheophyte homologs. However, MpPBLc clusters together with a single PBL paralog from *Anthoceros agrestis*, *Selaginella moellendorffii*, and *Arabidopsis*, suggesting that those PBLs are more divergent to other land plant PBLs. Based on the phylogeny, we considered MpPBLa and MpPBLb to be the major PBL isoforms, and MpPBLc to be a divergent PBL isoform in *Marchantia*. We next interrogated publicly available expression data[15] and found that the two major isoforms share a broad expression pattern across tissues and development stages and in response to various treatments (Figure S2A). The transcript abundance of Mp*PBLc* is relatively low compared to the other two Mp*PBLs* (except in the antheridium), suggesting a potential role for MpPBLc in sexual reproduction.

Please cite this article in press as: Chu et al., Conservation of the PBL-RBOH immune module in land plants, Current Biology (2023), https://doi.org/10.1016/j.cub.2023.01.050

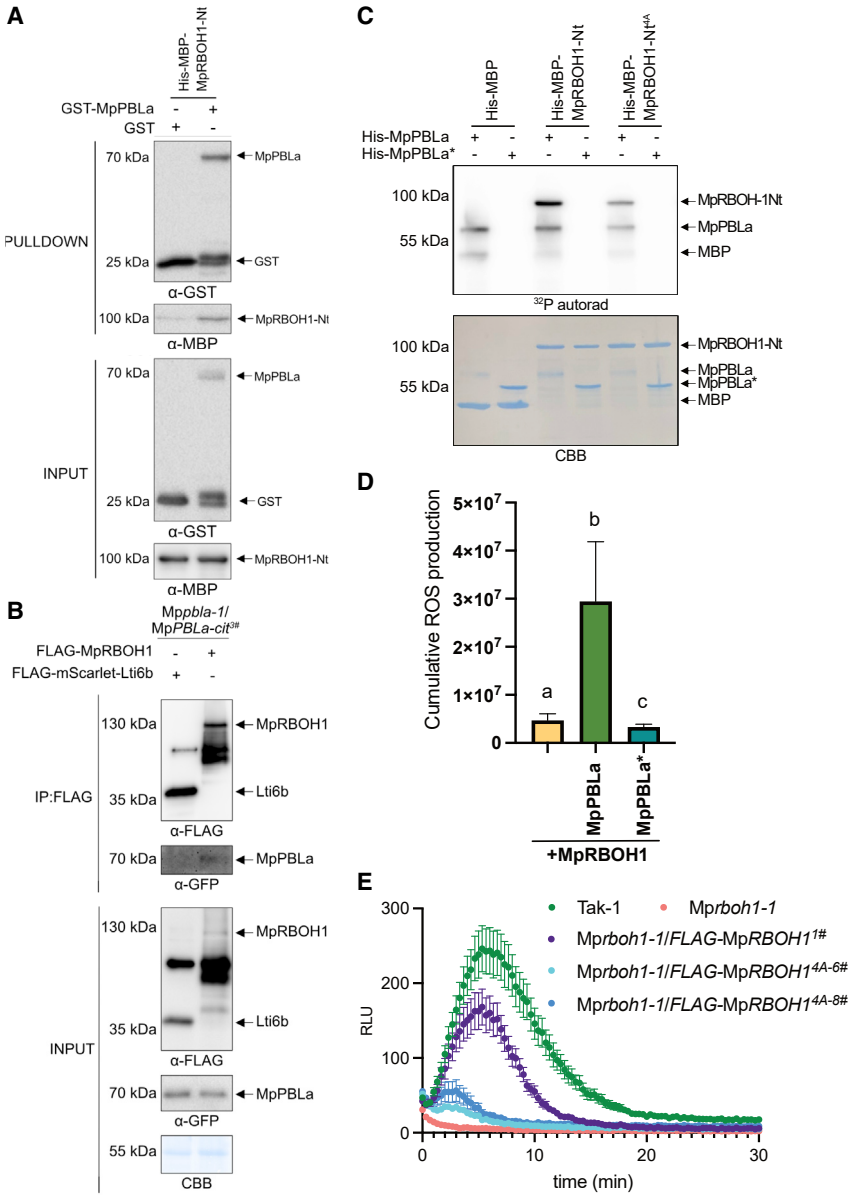

Figure 3. MpPBLa activates MpRBOH1 via N-terminal phosphorylation

(A) MpPBLa directly interacts with the MpRBOH1-Nt *in vitro*. Pull-down assay of His-MBP-tagged N-terminal fragments of MpRBOH1-Nt with GST-tagged MpPBLa. Free GST served as negative control.

(B) CoIP of MpPBLa-citrine after transient expression of FLAG-MpRBOH1 in Mp*pbla*/pro*35S*::Mp*PBLa-cit*[3#]. FLAG-mScarlet-Lti6b served as negative control for MpPBLa association. CoIP was repeated 3 times with similar results.

(C) MpPBLa phosphorylates S-X-X-L motif sites within MpRBOH1-Nt. Autoradiogram of *in vitro* kinase assay of His-MBP-tagged N-terminal fragments of MpRBOH1-Nt or MpRBOH1-Nt[4A] with WT or kinase-dead MpPBLa.

(D) MpPBLa activates MpRBOH1 in HEK293T cells. Cells were transfected with the indicated plasmid combinations. The phosphatase inhibitor Calyculin-A was added to the cells to stimulate PBL induced RBOH activation. Values correspond to the cumulative ROS production over last 5 min of recording. Error bars represent SE. Equal letters at the top of the panel indicate $p > 0.05$, one-way ANOVA and a post hoc Tukey test. The assay was performed 3 times with similar results.

(E) Chitin (0.1 mg/mL)-induced ROS production on 4-week-old *Marchantia* thallus discs in Tak-1, Mp*rboh1-1*, and Mp*rboh1-1* expressing MpRBOH1 or MpRBOH1[4A] fused with an N-terminal FLAG tag under the control of the 35S promoter. Values correspond to the mean of 12 samples (±SE) and are expressed in RLU. Experiments were performed 3 times with similar results.

See also Figure S3.

To study the function of MpPBLs in chitin-induced ROS production, we tried to generate knockout mutants for the two major isoforms of MpPBLs. Several alleles were obtained for Mp*PBLa* (Figure S2B), but we failed to isolate knockout mutants for Mp*PBLb* despite using multiple sets of guide RNAs. Besides plant immunity, PBLs regulate various developmental and reproductive processes in *Arabidopsis*.[23] It is thus possible that MpPBLb may have a critical role in the regulation of plant growth and development, and that its knockout mutants are therefore lethal. However, multiple, independent Mp*pbla* lines were not able to produce ROS in response to chitin treatment (Figure 2B), reminiscent of Mp*rboh1* mutants. To test whether MpPBLa kinase activity is required for chitin-triggered ROS production, we expressed the wild-type or kinase-dead (MpPBLa*, D228N) version of MpPBLa in Mp*pbla-1* background. The loss of ROS production of Mp*pbla-1* in response to chitin treatment was rescued by the expression of wild-type MpPBLa, but not the kinase-dead version (Figures 2C and S2C). Together, these data demonstrate that MpPBLa is required for chitin-induced ROS production in a kinase-activity-dependent manner.

Previous studies in angiosperm species revealed only quantitative defects in pattern-triggered ROS production in single, double, or higher-order *bik1* or *pbl* knockout mutants,[1,2,24,25] suggesting extensive genetic redundancy within the PBL family, which is further underscored by the targeting of multiple PBL family members by various pathogen-derived effectors.[2,26] Notably, the size of PBL family is considerably small in *Marchantia* (3 versus 46 of *Arabidopsis*). In keeping with the much less redundant MpPBL family, chitin-triggered ROS was completely abolished by loss of a single MpPBL, demonstrating the utility of *Marchantia* as a genetically tractable study system for plant immune signaling.

Interestingly, Mp*pbla* mutants show defects in thallus development but still produce rhizoids (Figures S2D and S2E). Notably, different PBLs regulate diverse plant growth and developmental processes in *Arabidopsis*, such as SCHENGEN 1 (SGN1)/PBL15 in Casparian strip formation,[27] or PBL34/35/36 in root quiescent center stem cell maintenance.[28] It will be of interest to dissect the potential regulatory roles of MpPBLa in plant growth and development in future studies.

Please cite this article in press as: Chu et al., Conservation of the PBL-RBOH immune module in land plants, Current Biology (2023), https://doi.org/10.1016/j.cub.2023.01.050

CellPress
OPEN ACCESS

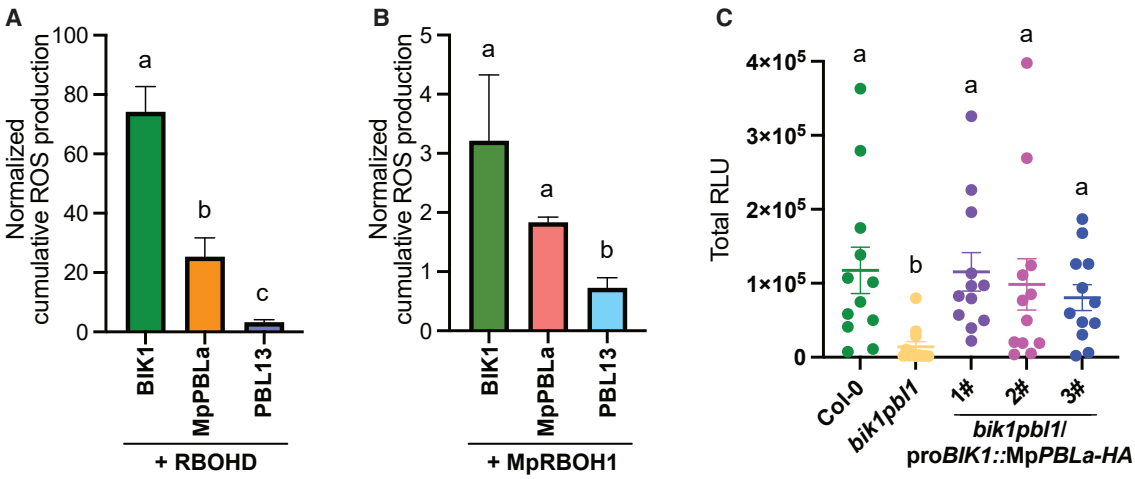

Figure 4. Conservation of PBL-RBOH module between *Arabidopsis* and *Marchantia*

(A) MpPBLa activates RBOHD in HEK293T cells.

(B) BIK1 activates MpRBOH1 in HEK293T cells. Cells were transfected with the indicated plasmid combinations. The phosphatase inhibitor Calyculin-A was added to the cells to stimulate PBL induced RBOH activation. Values correspond to the cumulative ROS production in the cells transfected with indicated PBL-RBOH combination normalized to the cells transfected with RBOH alone over last 5 min of recording (25 min). Error bars represent SE. Equal letters at the top of the panel indicate $p > 0.05$, one-way ANOVA and a post hoc Tukey test. The assay was performed 3 times with similar results.

(C) Chitin (0.1 mg/mL)-induced ROS production on 4-week-old *Arabidopsis* discs in Columbia-0, *bik1 pbl1*, and *bik1 pbl1* expressing MpPBLa fused with a C-terminal HA tag under the control of the native *BIK1* promoter. Scatter plots represent the total RLU (Total RLU) over a 30-min measurement, and horizontal bars and crosses represent mean and SE, $n = 12$. Equal letters at the top of the panel indicate $p > 0.05$, one-way ANOVA and a post hoc Dunn's test. Experiments were performed 3 times with similar results.

See also Figure S3.

MpRBOH1 is a *bona fide* substrate of MpPBLa

RBOHD is activated by BIK1 and related PBLs through direct interaction with and phosphorylation of RBOHD N terminus.[4,5,29] Given the shared phenotype of Mp*pbla* and Mp*rboh1* mutants in chitin-triggered ROS response, we hypothesized that MpPBLa similarly activates MpRBOH1 via phosphorylation. *In vitro* pull-down assays with recombinant maltose binding protein (MBP)-tagged MpRBOH1 N terminus (MpRBOH1-Nt) and GST-tagged MpPBLa also showed that MpRBOH1-Nt specifically interacted with MpPBLa (Figures 3A and S3A). We further performed co-immunoprecipitation (coIP) assays in *Marchantia*, which demonstrate that MpPBLa-citrine associated with FLAG-MpRBOH1 but not the plasma membrane marker Lti6b *in planta* (Figure 3B). We next performed *in vitro* kinase assays, which confirmed that MpPBLa can *trans*-phosphorylate MpRBOH1-Nt (Figure 3C). In *Arabidopsis*, BIK1 specifically phosphorylates several [S/T]-X-X-L motifs in the N terminus of RBOHD and these motifs are also present in RBOHD orthologs in different plant species.[5] Notably, similar motifs are conserved in the N terminus of MpRBOH1 (Figure S3B). To confirm the specificity of MpRBOH1 phosphorylation by MpPBLa, we performed *in vitro* kinase assays with MpRBOH1-Nt^{4A}, an MpRBOH1-Nt variant in which four MpPBLa-mediated phosphosites were mutated to non-phosphorylatable (alanine) residues. MpPBLa-mediated phosphorylation was strongly reduced when all four putative phosphosites in MpRBOH1-Nt were mutated to non-phosphorylatable versions (Figure 3C), and we subsequently confirmed two out of four by liquid chromatography-tandem mass spectrometry (LC-MS/MS) (Figure S3C). Together, these results indicate that MpPBLa directly interacts with and phosphorylates MpRBOH1-Nt at specific sites that are conserved among land plant RBOHs.

To test the effect of MpPBLa phosphorylation on MpRBOH1 function, we used a heterologous reconstitution system in human HEK293T cells.[30,31] The expression of MpRBOH1 alone resulted only in minor basal ROS generation that was comparable to that of cells transfected with an empty vector control. When MpRBOH1 was expressed together with the wild type, but not the kinase-dead MpPBLa, a significant increase in ROS production was observed (Figure 3D), confirming that MpPBLa activates MpRBOH1 in a kinase activity-dependent manner. To test the biological importance of MpRBOH1 phosphorylation by MpPBLa, we expressed in Mp*rboh1-1* a full-length MpRBOH1 variant harboring non-phosphorylatable (alanine) residue at MpPBLa-mediated phosphosites (MpRBOH1^{4A}). In contrast to wild-type MpRBOH1, MpRBOH1^{4A} failed to restore chitin-triggered ROS production (Figures 3E and S1F), demonstrating the functional importance of MpPBLa-mediated phosphorylation at these sites. In addition to PBL-mediated phosphorylation, RBOHD activation is regulated via phosphorylation at distinct sites by other kinases, such as Ca^{2+}-dependent protein kinases.[22] The observation that a minor ROS production could still be detected in lines expressing MpPBLa-mediated phosphosite mutant version of MpRBOH1 suggests additional MpRBOH1 regulatory mechanism(s) in *Marchantia*, which will need to be deciphered in future studies.

To further interrogate the conservation of this module between *Marchantia* and *Arabidopsis*, we reconstituted the reciprocal PBL-RBOH pathway in human HEK293T cells and measured ROS production indicative of the direct PBL-mediated activation of RBOH enzymatic activity. Both BIK1 and MpPBLa could activate their heterologous substrates (MpRBOH1 and RBOHD, respectively) (Figures 4A, 4B, and S3D). In contrast, co-expression

of PBL13, a previously identified *Arabidopsis* PBL family member that negatively regulates RBOHD activity,[32] did not induce discernible ROS production compared with expression of RBOHs alone (Figures 4A, 4B, and S3D). We next sought to examine the functional conservation of MpPBLa and BIK1 *in planta*. We transformed the *Arabidopsis bik1 pbl1* mutant with Mp*PBLa* under the control of the native *AtBIK1* promoter and observed complementation of *bik1pbl1* defective chitin-induced ROS production (Figures 4C and S3E). These results indicate the functional conservation of PBL family proteins in chitin-induced ROS production across land plants.

Aside from apoplastic ROS production, mitogen-activated protein kinase (MAPK) activation is another hallmark of early elicitor-induced immune signaling.[33,34] We thus investigated whether the MpPBLa-MpRBOH1 module is involved in chitin-induced MAPK activation in *Marchantia*. Chitin treatment induces an increase of MAPK activation in the wild-type Tak-1 plants, which was similar in Mp*pbla* and Mp*rboh1* mutants (Figure S3F). Multiple PBL family members have also been shown to regulate chitin-induced MAPK activation in *Arabidopsis* and rice,[24,35,36] and it is possible that chitin-induced MAPK activation and ROS production are regulated by distinct PBL family members in *Marchantia*. Though Mp*pbla* mutants had unaltered chitin-induced MAPK activation, we observed impaired chitin-induced expression of the immune marker gene Mp*WRKY22*[6] in Mp*pbla* (Figure S3G), suggesting that MpPBLa positively regulates immune gene expression in an MAPK-independent manner.

Our results demonstrate that MpRBOH1 is a *bona fide* substrate of MpPBLa, which is critical for PAMP-induced ROS production in *Marchantia* and highlight the striking conservation of this key regulatory step for plant NADPH activation. As *Arabidopsis* BIK1 controls different cellular immune outputs through direct phosphorylation of diverse substrates,[28,35,37–39] it will be interesting to see to which extent orthologous substrates in *Marchantia* are similarly regulated during immunity in this evolutionary model system. Future studies will also be needed to reveal the biological functions of MpRBOHs and MpPBLs identified in our study, in immunity and beyond.

STAR★METHODS

Detailed methods are provided in the online version of this paper and include the following:

SUPPLEMENTAL INFORMATION

Supplemental information can be found online at https://doi.org/10.1016/j.cub.2023.01.050.

ACKNOWLEDGMENTS

I.M. was supported by a long-term fellowship from the Human Frontier Science Program (LT000274/2019-L). T.A.D. was supported by postdoctoral fellowships from the European Molecular Biology Organization (#100-2017) and the Natural Sciences and Engineering Research Council of Canada (NSERC PDF-532561-2019). P.K. was supported by the EU Horizon 2020 Research and Innovation Program, Marie Skłodowska-Curie Actions (grant agreement no. 892398). This research was supported by the University of Zurich (C.Z.) and the Swiss National Science Foundation (grant agreement no. 31003A_182625 to C.Z.), and the Gatsby Charitable Foundation. The authors thank all members of the Zipfel lab for fruitful discussion and feedback on the manuscript. We also thank Hirofumi Nakagami for early discussions on chitin perception in *Marchantia*, as well as Jacqueline Monaghan and Pierre-Marc Delaux for discussions on immune signaling in *Marchantia*.

AUTHOR CONTRIBUTIONS

J.C., I.M., T.A.D., and C.Z. conceived and designed the project. J.C., I.M., T.A.D., P.K., and P.D. generated materials, performed experiments, and/or analyzed data. F.L.H.M. and C.Z. supervised the project. J.C. wrote the first draft of manuscript. All authors contributed to the final version of the manuscript.

DECLARATION OF INTERESTS

The authors declare no competing interests.

Received: June 22, 2022
Revised: December 10, 2022
Accepted: January 25, 2023
Published: February 15, 2023

REFERENCES

1. Lu, D., Wu, S., Gao, X., Zhang, Y., Shan, L., and He, P. (2010). A receptor-like cytoplasmic kinase, BIK1, associates with a flagellin receptor complex to initiate plant innate immunity. Proc. Natl. Acad. Sci. USA *107*, 496–501. https://doi.org/10.1073/PNAS.0909705107.
2. Zhang, J., Li, W., Xiang, T., Liu, Z., Laluk, K., Ding, X., Zou, Y., Gao, M., Zhang, X., Chen, S., et al. (2010). Receptor-like cytoplasmic kinases integrate signaling from multiple plant immune receptors and are targeted by a Pseudomonas syringae effector. Cell Host Microbe *7*, 290–301. https://doi.org/10.1016/J.CHOM.2010.03.007.
3. Veronese, P., Nakagami, H., Bluhm, B., AbuQamar, S., Chen, X., Salmeron, J., Dietrich, R.A., Hirt, H., and Mengiste, T. (2006). The membrane-anchored BOTRYTIS-INDUCED KINASE1 plays distinct roles in Arabidopsis resistance to necrotrophic and biotrophic pathogens. Plant Cell *18*, 257–273. https://doi.org/10.1105/TPC.105.035576.
4. Li, L., Li, M., Yu, L., Zhou, Z., Liang, X., Liu, Z., Cai, G., Gao, L., Zhang, X., Wang, Y., et al. (2014). The FLS2-associated kinase BIK1 directly

phosphorylates the NADPH oxidase RbohD to control plant immunity. Cell Host Microbe *15*, 329–338. https://doi.org/10.1016/J.CHOM.2014.02.009.

5. Kadota, Y., Sklenar, J., Derbyshire, P., Stransfeld, L., Asai, S., Ntoukakis, V., Jones, J.D., Shirasu, K., Menke, F., Jones, A., et al. (2014). Direct regulation of the NADPH oxidase RBOHD by the PRR-associated kinase BIK1 during plant immunity. Mol. Cell *54*, 43–55. https://doi.org/10.1016/J.MOLCEL.2014.02.021.
6. Gimenez-Ibanez, S., Zamarreño, A.M., García-Mina, J.M., and Solano, R. (2019). An evolutionarily ancient immune system governs the interactions between Pseudomonas syringae and an early-diverging land plant lineage. Curr. Biol. *29*, 2270–2281.e4. https://doi.org/10.1016/J.CUB.2019.05.079.
7. Bowman, J.L., Kohchi, T., Yamato, K.T., Jenkins, J., Shu, S., Ishizaki, K., Yamaoka, S., Nishihama, R., Nakamura, Y., Berger, F., et al. (2017). Insights into land plant evolution garnered from the Marchantia polymorpha genome. Cell *171*, 287–304.e15. https://doi.org/10.1016/j.cell.2017.09.030.
8. Yotsui, I., Matsui, H., Miyauchi, S., Iwakawa, H., Melkonian, K., Schlüter, T., Ibanez, S.G., Kanazawa, T., Nomura, Y., Stolze, S.C., et al. (2022). Genetic and phosphoproteomic basis of LysM-mediated immune signaling in Marchantia polymorpha highlights conserved elements and new aspect of pattern-triggered immunity in land plants. Preprint at bioRxiv. https://doi.org/10.1101/2022.12.28.521631.
9. Wong, H.L., Pinontoan, R., Hayashi, K., Tabata, R., Yaeno, T., Hasegawa, K., Kojima, C., Yoshioka, H., Iba, K., Kawasaki, T., et al. (2007). Regulation of rice NADPH oxidase by binding of Rac GTPase to its N-terminal extension. Plant Cell *19*, 4022–4034. https://doi.org/10.1105/TPC.107.055624.
10. Kobayashi, M., Ohura, I., Kawakita, K., Yokota, N., Fujiwara, M., Shimamoto, K., Doke, N., and Yoshioka, H. (2007). Calcium-dependent protein kinases regulate the production of reactive oxygen species by potato NADPH oxidase. Plant Cell *19*, 1065–1080. https://doi.org/10.1105/TPC.106.048884.
11. Yoshioka, H., Numata, N., Nakajima, K., Katou, S., Kawakita, K., Rowland, O., Jones, J.D.G., and Doke, N. (2003). Nicotiana benthamiana gp91phox homologs NbrbohA and NbrbohB participate in H2O2 accumulation and resistance to Phytophthora infestans. Plant Cell *15*, 706–718. https://doi.org/10.1105/TPC.008680.
12. Simon-Plas, F., Elmayan, T., and Blein, J.P. (2002). The plasma membrane oxidase NtrbohD is responsible for AOS production in elicited tobacco cells. Plant J. *31*, 137–147. https://doi.org/10.1046/J.1365-313X.2002.01342.X.
13. Nühse, T.S., Bottrill, A.R., Jones, A.M.E., and Peck, S.C. (2007). Quantitative phosphoproteomic analysis of plasma membrane proteins reveals regulatory mechanisms of plant innate immune responses. Plant J. *51*, 931–940. https://doi.org/10.1111/j.1365-313X.2007.03192.x.
14. Zhang, J., Shao, F., Li, Y., Cui, H., Chen, L., Li, H., Zou, Y., Long, C., Lan, L., Chai, J., et al. (2007). A Pseudomonas syringae effector inactivates MAPKs to suppress PAMP-induced immunity in plants. Cell Host Microbe *1*, 175–185. https://doi.org/10.1016/J.CHOM.2007.03.006.
15. Kawamura, S., Romani, F., Yagura, M., Mochizuki, T., Sakamoto, M., Yamaoka, S., Nishihama, R., Nakamura, Y., Yamato, K.T., Bowman, J.L., et al. (2022). MarpolBase expression: A web-based, comprehensive platform for visualization and analysis of transcriptomes in the liverwort Marchantia polymorpha. Plant Cell Physiol. *63*, 1745–1755. https://doi.org/10.1093/PCP/PCAC129.
16. Kubota, A., Ishizaki, K., Hosaka, M., and Kohchi, T. (2013). Efficient Agrobacterium-mediated transformation of the liverwort Marchantia polymorpha using regenerating thalli. Biosci. Biotechnol. Biochem. *77*, 167–172. https://doi.org/10.1271/BBB.120700.
17. Sugano, S.S., Shirakawa, M., Takagi, J., Matsuda, Y., Shimada, T., Hara-Nishimura, I., and Kohchi, T. (2014). CRISPR/Cas9-mediated targeted mutagenesis in the liverwort Marchantia polymorpha L. Plant Cell Physiol. *55*, 475–481. https://doi.org/10.1093/PCP/PCU014.
18. Marino, D., Dunand, C., Puppo, A., and Pauly, N. (2012). A burst of plant NADPH oxidases. Trends Plant Sci. *17*, 9–15. https://doi.org/10.1016/J.TPLANTS.2011.10.001.
19. Torres, M.A., Dangl, J.L., and Jones, J.D.G. (2002). Arabidopsis gp91phox homologues AtrbohD and AtrbohF are required for accumulation of reactive oxygen intermediates in the plant defense response. Proc. Natl. Acad. Sci. USA *99*, 517–522. https://doi.org/10.1073/PNAS.012452499.
20. Foreman, J., Demidchik, V., Bothwell, J.H.F., Mylona, P., Miedema, H., Torres, M.A., Linstead, P., Costa, S., Brownlee, C., Jones, J.D.G., et al. (2003). Reactive oxygen species produced by NADPH oxidase regulate plant cell growth. Nature *422*, 442–446. https://doi.org/10.1038/NATURE01485.
21. Honkanen, S., and Dolan, L. (2016). Growth regulation in tip-growing cells that develop on the epidermis. Curr. Opin. Plant Biol. *34*, 77–83. https://doi.org/10.1016/J.PBI.2016.10.006.
22. Kadota, Y., Shirasu, K., and Zipfel, C. (2015). Regulation of the NADPH oxidase RBOHD during plant immunity. Plant Cell Physiol. *56*, 1472–1480. https://doi.org/10.1093/PCP/PCV063.
23. Liang, X., and Zhou, J.-M. (2018). Receptor-like cytoplasmic kinases: central players in plant receptor kinase–mediated signaling. Annu. Rev. Plant Biol. *69*, 267–299. https://doi.org/10.1146/annurev-arplant-042817-040540.
24. Rao, S., Zhou, Z., Miao, P., Bi, G., Hu, M., Wu, Y., Feng, F., Zhang, X., and Zhou, J.M. (2018). Roles of receptor-like cytoplasmic kinase VII members in pattern-triggered immune signaling. Plant Physiol. *177*, 1679–1690. https://doi.org/10.1104/PP.18.00486.
25. Ranf, S., Eschen-Lippold, L., Fröhlich, K., Westphal, L., Scheel, D., and Lee, J. (2014). Microbe-associated molecular pattern-induced calcium signaling requires the receptor-like cytoplasmic kinases, PBL1 and BIK1. BMC Plant Biol. *14*, 374. https://doi.org/10.1186/S12870-014-0374-4.
26. Bastedo, D.P., Khan, M., Martel, A., Seto, D., Kireeva, I., Zhang, J., Masud, W., Millar, D., Lee, J.Y., Lee, A.H.Y., et al. (2019). Perturbations of the ZED1 pseudokinase activate plant immunity. PLoS Pathog. *15*, e1007900. https://doi.org/10.1371/JOURNAL.PPAT.1007900.
27. Fujita, S., De Bellis, D., Edel, K.H., Köster, P., Andersen, T.G., Schmid-Siegert, E., Dénervaud Tendon, V., Pfister, A., Marhavý, P., Ursache, R., et al. (2020). SCHENGEN receptor module drives localized ROS production and lignification in plant roots. EMBO J. *39*, e103894. https://doi.org/10.15252/EMBJ.2019103894.
28. DeFalco, T.A., Anne, P., James, S.R., Willoughby, A.C., Schwanke, F., Johanndrees, O., Genolet, Y., Derbyshire, P., Wang, Q., Rana, S., et al. (2022). A conserved module regulates receptor kinase signalling in immunity and development. Nat. Plants *8*, 356–365. https://doi.org/10.1038/s41477-022-01134-w.
29. Li, P., Zhao, L., Qi, F., Htwe, N.M.P.S., Li, Q., Zhang, D., Lin, F., Shang-Guan, K., and Liang, Y. (2021). The receptor-like cytoplasmic kinase RIPK regulates broad-spectrum ROS signaling in multiple layers of plant immune system. Mol. Plant *14*, 1652–1667. https://doi.org/10.1016/J.MOLP.2021.06.010.
30. Han, J.P., Köster, P., Drerup, M.M., Scholz, M., Li, S., Edel, K.H., Hashimoto, K., Kuchitsu, K., Hippler, M., and Kudla, J. (2019). Fine-tuning of RBOHF activity is achieved by differential phosphorylation and Ca 2+ binding. New Phytol. *221*, 1935–1949. https://doi.org/10.1111/NPH.15543.
31. Ogasawara, Y., Kaya, H., Hiraoka, G., Yumoto, F., Kimura, S., Kadota, Y., Hishinuma, H., Senzaki, E., Yamagoe, S., Nagata, K., et al. (2008). Synergistic activation of the Arabidopsis NADPH oxidase AtrbohD by Ca2+ and phosphorylation. J. Biol. Chem. *283*, 8885–8892. https://doi.org/10.1074/jbc.M708106200.
32. Lee, D.H., Lal, N.K., Lin, Z.D., Ma, S., Liu, J., Castro, B., Toruño, T., Dinesh-Kumar, S.P., and Coaker, G. (2020). Regulation of reactive oxygen species during plant immunity through phosphorylation and ubiquitination of RBOHD. Nat. Commun. *11*, 1838. https://doi.org/10.1038/s41467-020-15601-5.
33. Boller, T., and Felix, G. (2009). A renaissance of elicitors: perception of microbe-associated molecular patterns and danger signals by pattern-recognition receptors. Annu. Rev. Plant Biol. *60*, 379–406. https://doi.org/10.1146/ANNUREV.ARPLANT.57.032905.105346.

34. DeFalco, T.A., and Zipfel, C. (2021). Molecular mechanisms of early plant pattern-triggered immune signaling. Mol. Cell *81*, 4346. https://doi.org/10.1016/J.MOLCEL.2021.09.028.

35. Bi, G., Zhou, Z., Wang, W., Li, L., Rao, S., Wu, Y., Zhang, X., Menke, F.L.H., Chen, S., and Zhou, J.M. (2018). Receptor-like cytoplasmic kinases directly link diverse pattern recognition receptors to the activation of mitogen-activated protein kinase cascades in Arabidopsis. Plant Cell *30*, 1543–1561. https://doi.org/10.1105/TPC.17.00981.

36. Yamaguchi, K., Yamada, K., Ishikawa, K., Yoshimura, S., Hayashi, N., Uchihashi, K., Ishihama, N., Kishi-Kaboshi, M., Takahashi, A., Tsuge, S., et al. (2013). A receptor-like cytoplasmic kinase targeted by a plant pathogen effector is directly phosphorylated by the chitin receptor and mediates rice immunity. Cell Host Microbe *13*, 347–357. https://doi.org/10.1016/j.chom.2013.02.007.

37. Dindas, J., DeFalco, T.A., Yu, G., Zhang, L., David, P., Bjornson, M., Thibaud, M.C., Custódio, V., Castrillo, G., Nussaume, L., et al. (2022). Direct inhibition of phosphate transport by immune signaling in Arabidopsis. Curr. Biol. *32*, 488–495.e5. https://doi.org/10.1016/J.CUB.2021.11.063.

38. Thor, K., Jiang, S., Michard, E., George, J., Scherzer, S., Huang, S., Dindas, J., Derbyshire, P., Leitão, N., DeFalco, T.A., et al. (2020). The calcium-permeable channel OSCA1.3 regulates plant stomatal immunity. Nature *585*, 569–573. https://doi.org/10.1038/S41586-020-2702-1.

39. Lal, N.K., Nagalakshmi, U., Hurlburt, N.K., Flores, R., Bak, A., Sone, P., Ma, X., Song, G., Walley, J., Shan, L., et al. (2018). The receptor-like cytoplasmic kinase BIK1 localizes to the nucleus and regulates defense hormone expression during plant innate immunity. Cell Host Microbe *23*, 485–497.e5. https://doi.org/10.1016/J.CHOM.2018.03.010.

40. Sakuma, T., Nishikawa, A., Kume, S., Chayama, K., and Yamamoto, T. (2014). Multiplex genome engineering in human cells using all-in-one CRISPR/Cas9 vector system. Sci. Rep. *4*, 5400. https://doi.org/10.1038/SREP05400.

41. Shen, B., Zhang, W., Zhang, J., Zhou, J., Wang, J., Chen, L., Wang, L., Hodgkins, A., Iyer, V., Huang, X., et al. (2014). Efficient genome modification by CRISPR-Cas9 nickase with minimal off-target effects. Nat. Methods *11*, 399–402. https://doi.org/10.1038/NMETH.2857.

42. Ran, F.A., Hsu, P.D., Lin, C.Y., Gootenberg, J.S., Konermann, S., Trevino, A.E., Scott, D.A., Inoue, A., Matoba, S., Zhang, Y., et al. (2013). Double nicking by RNA-guided CRISPR Cas9 for enhanced genome editing specificity. Cell *154*, 1380–1389. https://doi.org/10.1016/J.CELL.2013.08.021.

43. Proost, S., and Mutwil, M. (2018). CoNekT: an open-source framework for comparative genomic and transcriptomic network analyses. Nucleic Acids Res. *46*, W133–W140. https://doi.org/10.1093/NAR/GKY336.

44. Notredame, C., Higgins, D.G., and Heringa, J. (2000). T-Coffee: A novel method for fast and accurate multiple sequence alignment. J. Mol. Biol. *302*, 205–217. https://doi.org/10.1006/JMBI.2000.4042.

45. Edgar, R.C. (2004). MUSCLE: multiple sequence alignment with high accuracy and high throughput. Nucleic Acids Res. *32*, 1792–1797. https://doi.org/10.1093/NAR/GKH340.

46. Nguyen, L.T., Schmidt, H.A., von Haeseler, A., and Minh, B.Q. (2015). IQ-TREE: A fast and effective stochastic algorithm for estimating maximum-likelihood phylogenies. Mol. Biol. Evol. *32*, 268–274. https://doi.org/10.1093/MOLBEV/MSU300.

47. Tamura, K., Stecher, G., and Kumar, S. (2021). MEGA11: Molecular Evolutionary Genetics Analysis Version 11. Mol. Biol. Evol. *38*, 3022–3027. version 11. https://doi.org/10.1093/MOLBEV/MSAB120.

48. Sauret-Güeto, S., Frangedakis, E., Silvestri, L., Rebmann, M., Tomaselli, M., Markel, K., Delmans, M., West, A., Patron, N.J., and Haseloff, J. (2020). Systematic tools for reprogramming plant gene expression in a simple model, Marchantia polymorpha. ACS Synth. Biol. *9*, 864–882. https://doi.org/10.1021/ACSSYNBIO.9B00511.

49. Lampropoulos, A., Sutikovic, Z., Wenzl, C., Maegele, I., Lohmann, J.U., and Forner, J. (2013). GreenGate - A novel, versatile, and efficient cloning system for plant transgenesis. PLOS One *8*, e83043. https://doi.org/10.1371/JOURNAL.PONE.0083043.

50. Waadt, R., Köster, P., Andrés, Z., Waadt, C., Bradamante, G., Lampou, K., Kudla, J., and Schumacher, K. (2020). Dual-reporting transcriptionally linked genetically encoded fluorescent indicators resolve the spatiotemporal coordination of cytosolic abscisic acid and second messenger dynamics in Arabidopsis. Plant Cell *32*, 2582–2601. https://doi.org/10.1105/TPC.19.00892.

51. Iwakawa, H., Melkonian, K., Schlüter, T., Jeon, H.-W., Nishihama, R., Motose, H., and Nakagami, H. (2021). *Agrobacterium* -Mediated transient transformation of *Marchantia* liverworts. Plant Cell Physiol. *62*, 1718–1727. https://doi.org/10.1093/pcp/pcab126.

52. Perez-Riverol, Y., Csordas, A., Bai, J., Bernal-Llinares, M., Hewapathirana, S., Kundu, D.J., Inuganti, A., Griss, J., Mayer, G., Eisenacher, M., et al. (2019). The PRIDE database and related tools and resources in 2019: improving support for quantification data. Nucleic Acids Res. *47*, D442–D450. https://doi.org/10.1093/NAR/GKY1106.

Please cite this article in press as: Chu et al., Conservation of the PBL-RBOH immune module in land plants, Current Biology (2023), https://doi.org/10.1016/j.cub.2023.01.050

CellPress
OPEN ACCESS

STAR★METHODS

KEY RESOURCES TABLE

REAGENT or RESOURCE	SOURCE	IDENTIFIER
Antibodies		
anti-GFP-HRP	Miltenyi Biotec	Cat#130-091-833; RRID: AB_247003
anti-HA-HRP	Roche	Cat#12013819001; RRID: AB_390917
anti-FLAG-HRP	Sigma	Cat#A8592; RRID: AB_439702
anti-MBP	NEB	Cat#E8032; RRID: AB_1559730
anti-GST	Upstate	Cat#06332
Anti-Rabbit IgG (whole molecule)–Peroxidase	Sigma	Cat#A0545; RRID: AB_257896
Anti-Mouse IgG (Fc specific)–Peroxidase	Sigma	Cat#A0168; RRID: AB_257867
anti-p44/42 MAPK (Erk1/2)	Cell Signaling	Cat#9102; RRID: AB_330744
Bacterial and virus strains		
E. coli BL21(DE3) Rosetta pLysS	Sigma	Cat#70956-M
Chemicals, peptides, and recombinant proteins		
6xHis-MpPBLa	This paper	N/A
6xHis-MpPBLa* (kinase-dead, D228N)	This paper	N/A
GST	This paper	N/A
GST-MpPBLa	This paper	N/A
6xHis-MBP-MpRBOH1Nt	This paper	N/A
6xHis-MBP-MpRBOH1Nt^{4A} (MpPBLa-mediated phosphor-site mutant)	This paper	N/A
DYKDDDDK Fab-Trap™ Agarose	Chromotek	Cat#ffa
RevertAid Reverse Transcriptase	Thermo	Cat#EP0441
PowerUP SYBR Green Master Mix	Thermo	Cat#A25741
ATP, [γ-^{32}P]- 3000Ci/mmol 10mCi/ml EasyTide	Perkin-Elmer	Cat# NEG502A250UC
HisPur Cobalt Resin	Thermo	Cat#89965
GST-Bind Resin	Millipore	Cat#70541
flg22	SciLight Biotechnology LLC	N/A
Peroxidase from horseradish	Sigma	Cat#77332
L-012	FUJIFILM	Cat#120-04891
Diphenyleneiodonium chloride	Sigma	Cat#D2926
Dulbecco's Modified Eagle's Medium	Sigma	Cat#D6429
PEI MAX® - Transfection Grade Linear Polyethylenimine Hydrochloride	Polysciences	Cat#24765
HBSS, calcium, magnesium, no phenol red	Gibco	Cat#15266355
Colloidal Chitin polysaccharide	Elicityl	Cat#GLU411
Protease Inhibitor Cocktail	Sigma	Cat#P9599
Cefotaxime sodium	Apollo Scientific	Cat#BIC0111
Chlorosulfuron	Supelco	Cat#34322
Hygromycin B solution	Panreac AppliChem	Cat#A2175
IGEPAL CA-630	Sigma	Cat#I3021
Deposited data		
Mass spectrometry proteomics data	This paper	PRIDE: PXD038639
Experimental models: Cell lines		
HEK293T	Widely distributed	N/A
Experimental models: Organisms/strains		
M. polymorpha Tak-1	Bowman et al.[7]	N/A

(*Continued on next page*)

Please cite this article in press as: Chu et al., Conservation of the PBL-RBOH immune module in land plants, Current Biology (2023), https://doi.org/10.1016/j.cub.2023.01.050

Continued

REAGENT or RESOURCE	SOURCE	IDENTIFIER
M. polymorpha (Tak-1) Mp*pbla*	This paper	N/A
M. polymorpha (Tak-1) Mp*rboh1*	This paper	N/A
M. polymorpha (Tak-1) Mp*rboh2*	This paper	N/A
M. polymorpha (Tak-1) Mp*pbla* *p35S*::Mp*PBLa-cit*	This paper	N/A
M. polymorpha (Tak-1) Mp*pbla* *p35S*::Mp*PBLa*-cit*	This paper	N/A
M. polymorpha (Tak-1) Mp*rboh1* *p35S*::*FLAG*-Mp*RBOH1*	This paper	N/A
M. polymorpha (Tak-1) Mp*rboh1 p35S*::*FLAG*-Mp*RBOH1*^{4A}	This paper	N/A
A. thaliana Col-0	Widely distributed	N/A
A. thaliana (Col-0) *bik1 pbl1*	Zhang et al.[2]	N/A
A. thaliana (Col-0) *bik1 pbl1 pBIK1*::Mp*PBLa-HA*	This paper	N/A
Oligonucleotides		
Primers for cloning and qPCR, see Table S1	This paper	N/A
Recombinant DNA		
pUAP4_MpPBLa	This paper	N/A
pUAP4_MpPBLa*	This paper	N/A
pUAP4_MpRBOH1	This paper	N/A
pUAP4_MpRBOH1^{4SA}	This paper	N/A
pGEX4T1_MpPBLa	This paper	N/A
pET28a_MpPBLa	This paper	N/A
pET28a_MpPBLa*	This paper	N/A
pOPINM_MpRBOH1Nt	This paper	N/A
pOPINM_MpRBOH1Nt^{4SA}	This paper	N/A
35S:FLAG-mScarlet-Lti6b	This paper	N/A
35S:FLAG-MpRBOH1	This paper	N/A
pMpGE018_MpPBLa	This paper	N/A
pMpGE018_MpRBOH1	This paper	N/A
pMpGE018_MpRBOH2	This paper	N/A
HyR; p35S::FLAG-MpRBOH1	This paper	N/A
HyR; p35S::FLAG-MpRBOH1^{4SA}	This paper	N/A
HyR; p35S::MpPBLa-citrine	This paper	N/A
HyR; p35S::MpPBLa*-citrine	This paper	N/A
HyR; pAtBIK1::MpPBLa-HA	This paper	N/A
pGGHEK_MpPBLa-2xStrepII	This paper	N/A
pGGHEK_HEK293-MpPBLa*-2xStrepII	This paper	N/A
pGGHEK_2xStrepII-MpRBOH1	This paper	N/A
pGGHEK_2xStrepII-AtRBOHD	This paper	N/A
pGGHEK_BIK1-2xStrepII	This paper	N/A
pGGHEK_PBL13-2xStrepII	This paper	N/A
Software and algorithms		
GraphPad Prism	GraphPad	v8.0.1
MEGA	MEGA	v11
Jalview	Jalview	v2.11.0
MS Convert	Proteowizard	N/A
Scaffold	Proteome Software	v.5.0.0
Mascot Daemon	Matrixscience	N/A

Please cite this article in press as: Chu et al., Conservation of the PBL-RBOH immune module in land plants, Current Biology (2023), https://doi.org/10.1016/j.cub.2023.01.050

CellPress
OPEN ACCESS

RESOURCE AVAILABILITY

Lead contact

Further information and requests for resources and reagents should be directed to and will be fulfilled by the lead contact, Cyril Zipfel (cyril.zipfel@botinst.uzh.ch).

Materials availability

Materials generated in this study are available from the lead contact without restrictions.

Data and code availability

- The mass spectrometry proteomics data have been deposited to the ProteomeXchange Consortium.
- This paper does not report original code.
- Any additional information required to reanalyze the data reported in this paper is available from the lead contact upon request.

EXPERIMENTAL MODEL AND SUBJECT DETAILS

Marchantia polymorpha accession Takaragaike-1 (Tak-1; male) was used in this study as the wild-type (WT). Marchantia gemmae were grown on half-strength Gamborg's B5, 1 % agar medium under continuous light (50-60 μmol m^{-2} s^{-1}) at 20 °C or as specified.

For ROS production assays, Marchantia gemmae were grown on half-strength Gamborg's B5, 1 % agar with a day/night cycle of 10 h:14 h at 21 °C and 16 °C.

Arabidopsis mutants and transgenic lines were in Col-0 background. All seeds were surface sterilized, sown on MS media containing 1% (w/v) sucrose, stratified for 2 days in the dark at 4°C, and moved to growth chamber with conditions 16 h day/8 h night at respectively 22°C/18°C and 120 μmol m^{-2} s^{-1}. 10-day-old seedlings were transplanted into soil and grown with a day/night cycle of 10 h:14 h at 21 °C and 16 °C.

HEK293T cells were cultivated in Dulbecco's modified Eagle's medium (DMEM) with 4.5 g/L Glucose, L-Glutamineglutamine and sodium pyruvate (Lonza) enriched with 10% fetal bovine serum at 5% CO_2 and 37°C.

METHOD DETAILS

Plant transformation and CRISPR–Cas9^{D10A} nickase-mediated mutagenesis

Marchantia was transformed following the cut-thalli transformation method as described.[16] Four different gRNAs (Table S1) were cloned into the BsaI site of pMpGE_En04, pBC-GE12, pBC-GE23 or pBC-GE34. The four gRNAs cassettes cloned into pMpGE_En04 were then transferred into pMpGE018 binary vector carrying the Cas9^{D10A} (nickase)[40–42] by LR reaction (Invitrogen). The individual destination vector was transformed into *Agrobacterium tumefaciens* strain GV3101. Marchantia cut-thalli (Tak-1) were transformed, and transformants were selected on chlorsulfuron, genotyped and sequenced. The expression of fusion protein in complementation lines of Mp*ppbla* or Mp*rboh1* mutants were analyzed by western blot. Total proteins were extracted with 6x SDS sample buffer. Samples were separated by SDS-PAGE, transferred to PVDF, and imaged by blotting with anti-FLAG (HRP-conjugated B-2, Sigma A8592, 1:5000 dilution) or anti-GFP (HRP-conjugated, MACS 130-091-933, 1:5000 dilution). *A.tumefaciens*-mediated Arabidopsis transformation was performed as previously described.[28] Transgenic lines were selected on hygromycin selection media (25 mg/L).

Gene identification and phylogenetic analyses

Sequences of Marchantia gene and protein were obtained from www.marchantia.info. Sequences of proteins used for analysis were retrieved from Phytozome, except for *Picea abies* from https://evorepro.sbs.ntu.edu.sg/.[43] All sequences were aligned with MUSCLE or T-COFFEE.[44,45] The phylogenetic analysis was performed by IQ-TREE or MEGA[46] based on PhyML[47] with a bootstrap analysis of 1000 replicates.

ROS production assays

For assays with Marchantia thalli, 12 thalli discs (approximately 4-mm diameter) from 4-week-old Marchantia plants growing in a KKD Hiros chamber (Clitec) with a day/night cycle of 10 h:14 h at 21 °C and 16 °C were sampled with a biopsy punch and incubated overnight in sterile water. The water was replaced with the solution containing 0.5 μM L-012, 10 μg/mL horseradish peroxidase (HRP), 0.1 mg/mL chitin (Colloidal Chitin polysaccharide, Elicityl) or 100 nM flg22 (SciLight Biotechnology LLC). DPI treatment was performed as previously described[27] with modifications accordingly. The overnight incubation water was replaced with the 10 μM DPI solution (Sigma) or sterile water, and discs were incubated for 3 h before replacing with the elicitor solution. For the preparation of chitin solution, the desired amount of Colloidal Chitin polysaccharide was weighted, and sterile water was added to achieve the working concertation. The chitin solution was mixed by vortexing before adding L-012 and HRP. Luminescence was captured over 30 min in 20-s intervals with a Photek camera (East Sussex). ROS production assays in Arabidopsis leave discs were conducted as previously described.[5]

Please cite this article in press as: Chu et al., Conservation of the PBL-RBOH immune module in land plants, Current Biology (2023), https://doi.org/10.1016/j.cub.2023.01.050

Molecular cloning

The coding sequence of Mp*PBLa* and Mp*RBOH1* were amplified from Tak-1 cDNA, and cloned into pUAP4 as described. Site-direct mutagenesis was performed with the primers provided in Table S1 to generate the Cas9-resistant version of Mp*PBLa* and Mp*RBOH1*, the kinase-dead version of Mp*PBLa*, and the phospho-dead version of Mp*RBOH1*. Mp*PBLa* or Mp*RBOH1* variants were cloned into the level 0 vector pUAP4, and further subcloned into level 1 or 2 binary constructs.[48] Sequences encoding MpPBLa and the N terminus of MpRBOH1 were cloned into pOPINM using InFusion (Takara). Mp*PBLa* was cloned into EcoRI/NotI-digested pGEX4T1 using the primers provided in Table S1. For expression in HEK293T cells, coding regions of MpRBOH1 and MpPBLa were cloned into GreenGate entry vector pGGC[49] and assembled with either N-terminal (for MpRBOH1) or C-terminal (for MpPBLa) 2xStrepII tag into the destination vector pGGHEK.[50]

Transient expression

Agrobacterium-mediated transient expression of Marchantia was performed as previously described.[51] Thalli of 3-week-old M*ppbla-1*/pro*35S*::Mp*PBLa-cit* were infiltrated with *A. tumefaciens* carrying constructs as indicated in figure captions.

Protein extraction and co-immunoprecipitation

For co-IP, Marchantia thalli were harvested 3 days post-infiltration. Tissue was frozen and ground in liquid nitrogen. Protein extraction and immunoprecipitation were performed as described previously[37] using DYKDDDDK Fab-Trap™ Agarose (Chromotek). Proteins were separated by SDS-PAGE and blotted onto PVDF membrane. Membranes were blocked and probed in TBST-5 % non-fat milk using blotting with anti-FLAG (HRP-conjugated B-2, Sigma A8592, 1:5000 dilution) or anti-GFP (HRP-conjugated, MACS 130-091-933, 1:5000 dilution).

Recombinant protein expression and purification

All recombinant proteins used in this study were expressed in *Escherichia coli* strain BL21(DE3) Rosetta pLysS. MpPBLa, MpPBLa* (kinase-dead, D228N), the N-terminus, and the C-terminus of MpRBOHa were all expressed as 6xHis-MBP fusions. MpPBLa was also expressed as a GST fusion protein. Recombinant proteins were affinity-purified using HisPur Cobalt Resin (Thermo) or GST-Bind Resin (Millipore) for 6xHis-MBP, and GST fusions, respectively.

In vitro pulldown assays

Approximately 6 μg of bait and 10 μg of prey proteins were mixed to 100 μL final volume in the binding buffer (25 mM Tris-Cl pH 7.4, 100 mM NaCl, 0.2 % Triton-X100, 1 mM DTT). Thirty microliters were taken out as 'input'. Fifty microliters of GST-Bind Resin (Millipore) were added to the tube with the binding buffer topping up to a final volume of 500 μL. Samples were mixed on a rotator at room temperature (RT) for 30 min. The enriched proteins were eluted with 50 μL SDS-loading dye ('pulldown') from the resin after washing four times with the binding buffer. Samples were separated by SDS-PAGE, transferred to PVDF, and imaged by blotting with anti-GST (Upstate 06332, 1:5000 dilution), or anti-MBP (NEB E8032, 1:2000 dilution) antibodies following by anti-Rabbit (Sigma A0168, 1:10000 dilution), or anti-Mouse (Sigma A0545, 1:10000 dilution) secondary antibodies.

In vitro kinase assays

Approximately 1 μg of kinase and was incubated with approximately 2 μg of substrate protein in kinase buffer (25 mM Tris-Cl pH 7.4, 5 mM $MnCl_2$, 5 mM $MgCl_2$, 1 mM DTT). Five micromolar of ATP plus 0.5 μCi ^{32}P-γ-ATP in a final reaction volume of 30 μL were added to the tube to initiate the reaction. Reactions were incubated at RT for 30 min and terminated by addition of SDS-loading dye following by heating at 70 °C for 10 min. Proteins were resolved by SDS-PAGE, transferred to PVDF membrane, and stained with Coomassie brilliant blue G-250. Autoradiographs were imaged using an Amersham Typhoon phosphorimager (GE Healthcare).

ROS production assay in HEK293T cells

Activity of MpRBOH1 in HEK293T cells was assessed as described previously.[27] In brief, before transfection, cells were seeded into white, tissue-culture treated 96 well plates (Greiner). Individual wells were transformed with the indicated expression constructs using 50 ng of MpRBOH1 plasmids and 30 ng of MpPBLa plasmids, respectively, using the PEI-MAX® (Polysciences) transfection reagent. Forty-eight hours after transfection, cultivation media was aspirated, and cells were washed with Hank's Balanced Salt Solution (HBSS) (Gibco). Afterwards, 100 μL of a measurement buffer consisting of HBSS with 62 μM L-012 and 60 μg/ml HRP was added to each well. Cells were stimulated with 0.1 μM of the phosphatase inhibitor Calyculin-A and ROS production was measured using a Spark® multimode microplate reader (TECAN) over a 25-min measurement.

RNA extraction and real-time (RT) quantitative PCR analysis

Total RNA was extracted from target tissues by FavorPrep Plant Total RNA Purification Mini Kit (Favorgen) following the manufacturer's instruction. First-strand cDNA synthesis was performed by using 1 μg of DNA-free RNA sample with RevertAid First Strand cDNA Synthesis Kit (Thermo Fisher Scientific) according to the manufacturer's protocol. For RT-qPCR analysis, diluted cDNA was used as the template for PowerUp SYBR Green (Applied biosystems) with the primers provided in Table S1. Data were analyzed using the ΔΔCT method and normalized against the expression level of Mp*UBOX*.[6] For each sample, three biological replicates were performed, and each biological replicate contained three technical replications.

Please cite this article in press as: Chu et al., Conservation of the PBL-RBOH immune module in land plants, Current Biology (2023), https://doi.org/10.1016/j.cub.2023.01.050

MAPK activation assay in Marchantia thalli

Two-week-old Marchantia thalli grown on half-strength Gamborg's B5, 1 % agar medium were transferred to liquid medium 24 h before treatment. Individual thalli were vacuum infiltrated with 0.1 mg/mL chitin (Colloidal Chitin polysaccharide, Elicityl) and harvested at each time point as indicated in figure captions. Total proteins were extracted and analyzed by SDS-PAGE and immunoblotting as described above with p44/42 MAPK (Erk1/2) antibody (Cell Signaling).

LC-MS/MS Analysis

LC-MS/MS analysis was performed as previously described[28] with minor differences. Approximately 35% of each sample was analysed using an Orbitrap Fusion Tribrid Mass Spectrometer (Thermo Fisher Scientific) coupled to a U3000 nano-UPLC (Thermo Fisher Scientific). The mass spectrometry proteomics data have been deposited to the ProteomeXchange Consortium via the PRIDE[52] partner repository with the dataset identifier PRIDE: PXD038639.

Data processing and peptide identification

Peak lists in the form of Mascot generic files were prepared from raw data files using MS Convert (Proteowizard) and sent to a peptide search on Mascot server v.2.8.0 using Mascot Daemon (Matrix Science) against an in-house constructs and contaminants database and the *E. coli* K12 protein database. Tryptic peptides with up to one possible mis-cleavage and charge states +2 and +3 were allowed in the search. The following peptide modifications were included in the search: carbamidomethylated cysteine (fixed), oxidized methionine (variable) and phosphorylated serine, threonine and tyrosine (variable). Data were searched with a monoisotopic precursor and fragment ion mass tolerance 10 ppm and 0.8 Da respectively. Decoy database was used to validate peptide sequence matches. Mascot results were combined in Scaffold v.5.0.0 (Proteome Software) and filtered to show only phospho-peptides. Peptide and protein identifications were accepted if peptide probability and protein threshold was $\geq$80.0% and 95% respectively. Phospho-site specificity was then confirmed by eye. Data were then exported to Excel (Microsoft) for further processing. For each phospho-peptide, spectral counts from all biological replicates were summed. Spectral counts from mis-cleaved peptides identifying the same phosphorylation site were then summed to give final spectral counts for each site.

QUANTIFICATION AND STATISTICAL ANALYSIS

Data were visualized using GraphPad and Jalview programs as described in method details. Statistical tests, n values, and significance cutoffs are described in figure legends and/or method details.